

Chapter 7

Magnetically controlled gravity for protein crystal growth

The occurrence of convective flows during crystal growth adversely affects crystal quality. Space-based crystal growth is therefore actively pursued, particularly for protein crystals, because buoyancy-driven convection is suppressed in microgravity. Here we demonstrate that magnetic fields can be used to tune the effective gravity from 1 g to -0.15 g during the growth of diamagnetic lysozyme crystals, and that convection can be damped, stopped and even reversed. This method provides a versatile and accessible way to realise an Earth-based tunable gravity environment for crystal growth, opening new avenues to optimise crystal quality.

7.1 Introduction

On earth, crystal growth from a supersaturated solution is accompanied by convection in the liquid; an effect often detrimental to crystal quality [1]. The convection is caused by buoyancy forces due to gravity, driven by the inherent density variations in the liquid near the growing crystal surface. For protein crystals a high quality is required for X-ray structure determination at high resolution [1, 2], which is of great biotechnological and pharmacological importance. However, protein crystals of high quality are difficult to grow, largely due to adverse effects of convection, which maintains a high growth rate and continuously supplies impurities to the surface of the crystals. For this reason much effort has been put in examining the virtues of space-based microgravity for protein crystal growth [1–3]. However, whether zero gravity is the ideal growth condition still is an open question and the attractive solution for optimising crystal quality, i.e. to be able to continuously tune the gravity, and thus convection, is yet to be achieved.

It has been shown that gradient magnetic fields can influence convective flows in paramagnetic fluids [4–6], and to apply the same approach to seemingly non-magnetic proteins is appealing, since in fact all diamagnetic materials can be magnetically levitated [7, 8]. For diamagnetic substances, the magnetic moment (\mathbf{m}) is proportional to the applied magnetic field (\mathbf{B}): $\mathbf{m} = \chi\mathbf{B}$, where χ is the magnetic susceptibility. A gradient magnetic field therefore leads to a magnetic force per unit volume given by $\mathbf{F}_{magn.} = \frac{\chi}{\mu_0}\mathbf{B}\nabla\mathbf{B}$, with μ_0 the magnetic permeability of free space, and pointed towards regions of low magnetic field.

The best known illustration of this effect is magnetic levitation, where the magnetic force counteracts the force of gravity $\mathbf{F}_{grav.} = \rho\mathbf{g}$ (ρ is the mass density and \mathbf{g} is the gravitational acceleration), causing the object to float [7–9]. Magnetic levitation has been demonstrated for a large variety of diamagnetic materials [10–12], and even for living creatures [9]. The required condition for levitation is given by: $B_z B'_z = -\rho\mu_0 g/\chi$, where B'_z is the derivative of B_z in the z , i.e. vertical, direction. For most non-metallic diamagnetic substances the ratio ρ/χ is similar [12, 13] and the necessary field gradient (expressed in

terms of $B_z B'_z$) is approximately $-1500 \text{ T}^2/\text{m}$.

The criterion for damping convection during crystal growth is quite different from that for levitation, because it relies on balancing buoyancy rather than gravitational force [5]. A growing crystal extracts solute from the solution and thus locally reduces the mass density of the solution. The diluted liquid close to the crystal surface will rise due to buoyancy, which leads to a convection pattern, comprising a thin (typically 0.1-0.3 mm) laminar flow boundary layer (depletion zone) and a so-called growth plume [14] on top of the crystal (Fig. 7.1a). Without convection this plume disappears, diffusion remains the sole means of mass transport and the depletion zone will expand to infinity (Fig. 7.1b). To suppress convection the buoyancy forces caused by differences in mass density ($\Delta\rho$) have to be opposed by magnetic buoyancy forces due to differences in magnetic susceptibility ($\Delta\chi$), giving $B_z B'_z = -\Delta\rho\mu_0g/\Delta\chi$ [5, 6]. For small variations in concentration of the solute, both the density and the susceptibility depend linearly on concentration, i.e., $\rho(c) = \alpha c + \rho_0$ and $\chi(c) = \beta c + \chi_0$, leading to:

$$B_z B'_z = \frac{\alpha}{\beta} \mu_0 g . \quad (7.1)$$

The suppression of buoyancy depends therefore on the concentration dependence of the mass density and susceptibility (α and β), and not on the mass density and susceptibility themselves, as for normal and magneto-Archimedes [15, 16] levitation. In the latter case diamagnetic objects are lifted in a paramagnetic host environment in a relatively low field gradient ($420 \text{ T}^2/\text{m}$), exploiting the large difference in susceptibility of object and host. In contrast, we need to balance buoyancy forces in a liquid with a *continuous* range of concentration dependent *diamagnetic* susceptibilities and mass densities, requiring very different values of the field gradient.

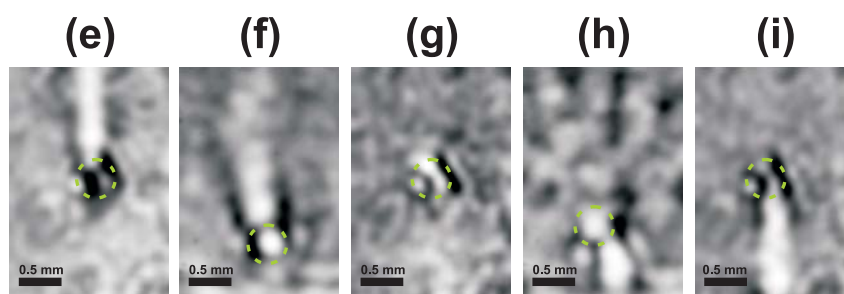
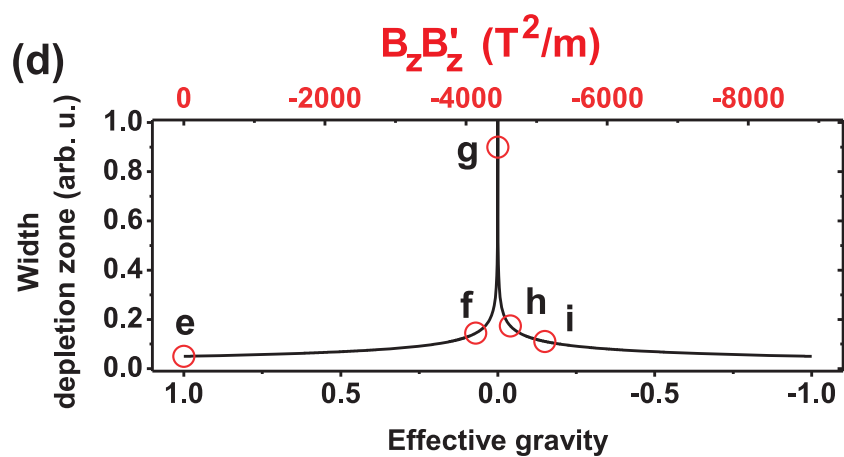
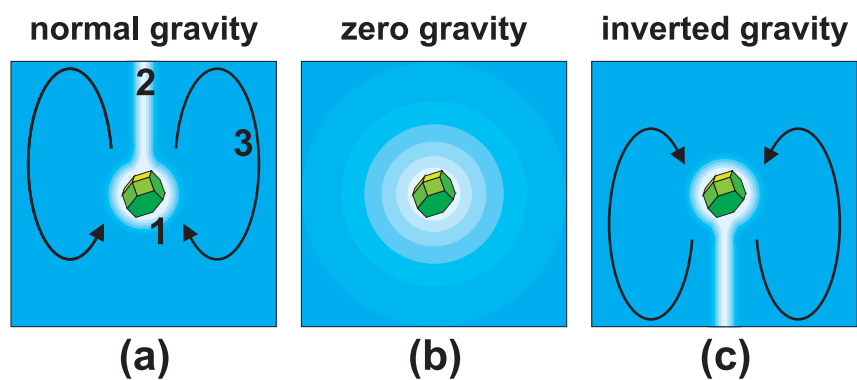
7.2 Experimental setup

We demonstrate the new method using the diamagnetic protein hen egg-white lysozyme (HEWL) for which crystallisation conditions have been well established and extensively investigated [17]. The experiments were performed in a

Figure 7.1: See page 121. Magnetically tuned gravity during crystal growth. (a) A growing crystal depletes its surrounding solution (1), leading to a growth plume (2) and convective flows (3). (b) At zero effective gravity convection is cancelled and the diffusion field expands. (c) In inverted gravity the buoyancy-driven convection is reversed, and a downward growth plume is formed. (d) Tuning of effective gravity is realised by changing the gradient magnetic field ($B_z B'_z$). G_{eff} affects the balance between convective and diffusive mass transport and determines the width of the depletion zone. (e)-(i) Experimental shadowgraphy images of a growing lysozyme crystal (indicated by the dashed green circles) in solution for G_{eff} ranging from -0.15 to 1.

33 T water-cooled resistive magnet with a bore diameter of 32 mm at the High Field Magnet Laboratory at the Radboud University Nijmegen. The magnet, fitted with a double-walled tube for temperature control by a thermostated water flow, contains a shadowgraphy [18] set-up for imaging convection patterns around the growing crystal (Fig. 7.2a). A glass cuvette (inner dimensions 8x4x18 mm³) with crystal and solution was placed at the position of maximum field gradient $|B_z B'_z|$ (red curve in Fig. 7.2b), for a given maximum field B_0 . The cuvette is illuminated from the side by a highly collimated beam of light from a halogen lamp, using an optical fibre in combination with a lens and a 75 μm pinhole, leading to an image on a CCD camera. Variations in the concentration of the fluid, like those between growth plume and bulk solution, lead to local differences in the refractive index, which appear as intensity variations in the image. The sensitivity to concentration differences scales with the degree of being out of focus [18].

We used hen egg-white lysozyme from Sigma-Aldrich (Lot nr. 094K-1454), which was dissolved and dialysed against a 0.05 M NaOAc/HOAc buffer solution of pH 4.5 at room temperature before use. Stock solution concentration was determined by UV absorption measurements at 281.5 nm [19]. Tetragonal lysozyme crystals were grown from a solution of 30 mg/ml HEWL, 0.685 M (or 4% w/v) NaCl and 0.05 M NaOAc/HOAc at pH 4.5 and 18 °C. Crystals



B_0	0	26.0	27.0	27.5	29.0 T
$B_z B'_z$	0	-4130	-4450	-4630	-5140 T ² /m
G_{eff}	1	0.07	0	-0.04	-0.15

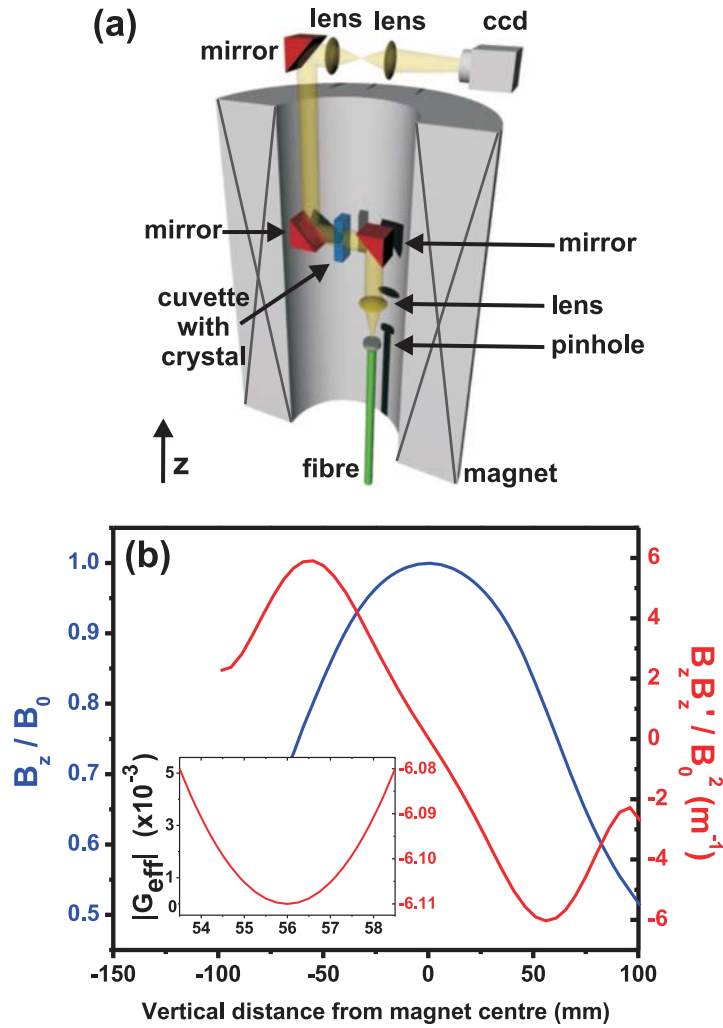


Figure 7.2: Experimental set-up for in-situ observation of convective fluid flows in a 33T magnet. (a) Schematic representation of the shadowgraphy insert used to visualise density variations in solutions. (b) Profiles of magnetic field and field times field gradient ($B_z B'_z$) scaled to a B_0 background field. The inset shows the $B_z B'_z$ profile around the optimum position and the corresponding effective gravity when convection is stopped. In this case, effective gravity ranges from 0 to $5 \times 10^{-3} g$ over 5 millimetres in height, which demonstrates that milligravity is sufficient to cancel convection.

were taken from the growth vessel and placed as a seed in the glass cuvette for the magnet experiments. The crystal was manipulated to the right spot on the glass wall of the cuvette to be in the field of view of the insert, after which the solution was removed and the cuvette was placed in a refrigerator at 4 °C for 20 minutes. As a result, the crystal is attached to the glass wall of the cuvette. Finally, the cuvette was refilled with the same solution as used during growth and placed in the insert for experiments.

7.3 Results and discussion

The condition for convection damping is determined by α and β in equation 7.1. For HEWL α is $0.303 \text{ kg m}^{-3} / \text{mg ml}^{-1}$ [20], and we have determined β to be $(-1.2 \pm 0.5) \times 10^{-9} \text{ ml/mg}$ using a magnetic susceptibility balance. Inserting these values in equation (7.1) we expect that convection is damped at $B_z B'_z = -3100 \pm 1500 \text{ T}^2/\text{m}$, which is significantly larger than the $-1500 \text{ T}^2/\text{m}$ needed for simple levitation of the bulk solution. Given the inaccuracy of this estimated field gradient, caused by the small and difficult to determine value of β , we determined the actual gradient field at which the growth plume disappears by using shadowgraphy. Figure 7.1e shows a growing HEWL crystal at zero field gradient, and the convection plume is clearly visible as a white streak rising upward from the crystal. In the picture the crystal itself is blurred because for shadowgraphy out-of-focus images have to be taken. The growth plume disappears, and thus convection is suppressed, at a gradient magnetic field of $-4450 \pm 30 \text{ T}^2/\text{m}$ (Fig. 7.1g). The value falls within our estimate using α and β , but is much higher than previously expected [5, 21] and requires the largest magnets currently available. In fact, this value for the gradient field accurately determines β as $(-0.84 \pm 0.06) \times 10^{-9} \text{ ml/mg}$.

This result unambiguously shows that gradient magnetic fields can create conditions on Earth that mimic those in space-based microgravity. Most importantly, however, is the fact that by changing the magnetic field strength the effective gravity for convection can be continuously varied. If we define

[22]

$$G_{\text{eff}} = 1 - \frac{\beta}{\alpha\mu_0g} B_z B'_z, \quad (7.2)$$

G_{eff} is expressed in terms of the Earth's gravitational acceleration g . $G_{\text{eff}} = 1$ at zero magnetic field, while convection is cancelled at a field gradient for which $G_{\text{eff}} = 0$. By varying the magnetic field we are able to change G_{eff} from 1 to -0.15, and as a result the convection is tuned from normal, with a growth plume upwards (Fig. 7.1e,f, via cancellation at $G_{\text{eff}}=0$ (Fig. 7.1g), to inverted with the growth plume downwards for negative values of G_{eff} (Fig. 7.1h,i).

The range of field gradients at which convection is stopped is quite small, $\pm 30 \text{ T}^2/\text{m}$ centred around $-4450 \text{ T}^2/\text{m}$, which corresponds to $B = 27 \text{ T}$ in the magnet we used. Decreasing (increasing) the magnetic field by only 0.1 T ($G_{\text{eff}} \approx \pm 0.005$) already results in appreciable convection and upward (downward) growth plumes. This strong effect is caused by the steep dependence of the balance between convective flow and mass diffusion on G_{eff} , which is reflected by the thickness of the depletion zone. For example, Fig. 7.1d shows the theoretically calculated, and for $\text{NiSO}_4 \cdot 6\text{H}_2\text{O}$ experimentally demonstrated [22], dependence of the thickness of the depletion zone δ on gravity. Since $\delta \propto |G_{\text{eff}}|^{-1/4}$ it diverges near zero, which implies that the field gradient has to be set quite precisely. Such a strong dependence also puts constraints on the spatial variation of G_{eff} within a magnet. From equation (7.2) we calculate G_{eff} as function of the position around the crystal using the experimental field profile (inset Fig. 7.2b), which shows that changes of G_{eff} over the relevant region are within ± 0.005 . Despite the precise condition on the required field gradient, *milligravity*, rather than microgravity [23], is sufficient to make convective transport slower than that due to diffusion, and successfully dampen convection.

To show that indeed the suppression of convection affects crystal growth, we have measured the growth rate of two lysozyme crystals, one at $G_{\text{eff}}=1$ (normal convection) and one at 0 (no convection), at otherwise identical conditions (Fig. 7.3). Here the same imaging set-up was used, but now with the crystal in focus to determine the position of its surface. The growth rate drops a factor of fifteen, from 30 ± 2 to $2 \pm 2 \text{ }\mu\text{m}$ per hour when convec-

tion is stopped and the depletion zone is expanded, which is similar to results obtained under space-based microgravity [24].

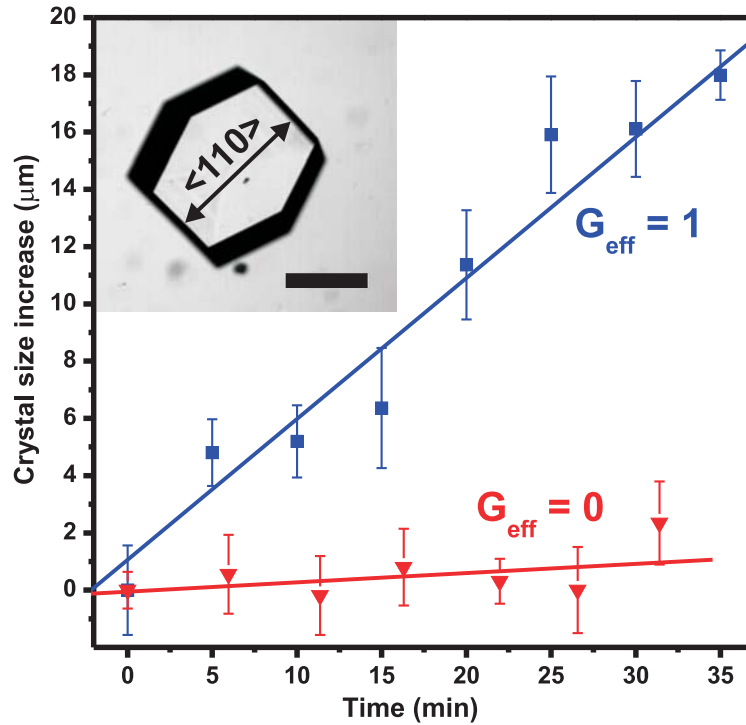


Figure 7.3: Growth rate of tetragonal hen egg-white lysozyme (HEWL) crystals at normal and zero effective gravity, G_{eff} . The squares (triangles) denote the increase in HEWL crystal size at a G_{eff} of 1 (0), obtained in the $\langle 110 \rangle$ direction, in a 30 mg/ml HEWL, 4% NaCl, 0.05 M NaOAc/HOAc solution at pH 4.5 and 18 °C. The growth rate at $G_{\text{eff}}=0$ is $2 \pm 2 \mu\text{m/hr}$ and is reduced by roughly a factor 15 compared to the growth rate at $G_{\text{eff}}=1$ of $30 \pm 2 \mu\text{m/hr}$. The inset shows a tetragonal HEWL crystal similar to those used in the experiments, and the $\langle 110 \rangle$ direction with respect to the morphology. The scale bar indicates 500 μm .

In contrast with other methods to suppress convection [25, 26], gradient magnetic fields offer a powerful way to tune the effective gravity during crystal growth under Earth-based conditions, with far easier access, availability,

and including in-situ observation. Especially for protein crystal growth this possibility is very attractive, since the tunability allows us to optimise the crystal quality by finding the right balance between mass transport towards the crystal and the incorporation rate of molecules at the crystal surface. The required gradient magnetic fields for suppression of convection are found to be in the 4000-5000 T²/m range, as expected from the concentration dependence of both mass density and magnetic susceptibility. Because density and susceptibility are closely related, we expect that this value is rather similar for most diamagnetic proteins, and possibly even for other diamagnetic compounds. For instance, we have found a value of (4070 ± 30) T²/m for potassium dihydrogen phosphate. We foresee that our determination of the proper conditions for which convection is suppressed will trigger the design and construction of dedicated magnets (possibly combined with paramagnetic field enhancers), that are capable of sustaining high field gradients for the several days that are needed to grow protein crystals.

Acknowledgements

The authors thank J. Rook, R. van Stijn and Mrs. J. van Oostrum for technical support and D. van Heijnsbergen for a critical reading of the manuscript. This work is part of the research programs of the 'Stichting voor Fundamenteel Onderzoek der Materie' (FOM), and the Council for the Chemical Sciences (CW), financially supported by the Netherlands Organisation for Scientific Research (NWO). K.T. was supported by the Japan Space Forum as part of the "Ground Based Research Announcement for Space Utilization".

References

- [1] E. H. Snell and J. R. Helliwel, Rep. Prog. Phys. **68**, 799 (2005).
- [2] A. Vergara *et al.*, Biophys. Chem. **118**, 102 (2005).
- [3] W. Littke and C. John, Science **225**, 203 (1984).

-
- [4] D. Braithwaite, E. Beaugnon, and R. Tournier, *Nature* **354**, 134 (1991).
- [5] N. Ramachandran and F. W. Leslie, *J. Cryst. Growth* **274**, 297 (2005).
- [6] P. W. G. Poodt *et al.*, *Appl. Phys. Lett.* **87**, 214105 (2005).
- [7] E. Beaugnon and R. Tournier, *Nature* **349**, 470 (1991).
- [8] A. Geim, *Physics Today* **51**, 36 (1998).
- [9] M. V. Berry and A. K. Geim, *Eur. J. Phys.* **18**, 307 (1997).
- [10] E. Beaugnon and R. Tournier, *J. Phys. III (Paris)* **1**, 1423 (1991).
- [11] J. S. Brooks *et al.*, *J. Appl. Phys.* **87**, 6194 (2000).
- [12] M. Motokawa *et al.*, *Physica B* **294-295**, 729 (2001).
- [13] J. F. Schenck, *Ann. N.Y. Acad. Sci.* **649**, 285 (1992).
- [14] P. J. Shlichta, *J. Cryst. Growth* **76**, 656 (1986).
- [15] Y. Ikezoe *et al.*, *Nature* **393**, 749 (1998).
- [16] A. T. Catherall *et al.*, *Nature* **422**, 579 (2003).
- [17] A. McPherson, *Crystallization of Biological Macromolecules* (Cold Spring Harbor Laboratory Press, New York, 1999).
- [18] G. S. Settles, *Schlieren and Shadowgraphy Techniques* (Springer, Berlin, 2001).
- [19] K. C. Aune and C. Tanford, *Biochemistry* **8**, 4579 (1969).
- [20] W. J. Fredericks *et al.*, *J. Cryst. Growth* **141**, 183 (1994).
- [21] N. I. Wakayama, *Jpn. J. Appl. Phys.* **44**, L833 (2005).
- [22] P. W. G. Poodt *et al.*, *Cryst. Growth Des.* **6**, 2275 (2006).
- [23] N. Ramachandran, C. R. Baugher, and R. J. Naumann, *Microgravity Sci. Technol.* **8**, 170 (1995).

- [24] F. Otalora *et al.*, Acta Crystallogr. **D58**, 1681 (2002).
- [25] M. C. Robert and F. Lefauchaux, J. Cryst. Growth **90**, 358 (1988).
- [26] D. C. Carter *et al.*, J. Appl. Crystallogr. **38**, 87 (2005).